Temperature dependent dielectric characteristics of PPY/Y_2O_3 composite

M. Riaz[a], M. Ali[b], F. Fareed[c], S. M. Ali[d,*], M. Alam[e]
[a]*Institute of physics, The Islamia university of Bahawalpur, Bahawalpur 63100, Pakistan*
[b]*Scool of Engineering and Digital Arts, University of Kent, Canterbury Kent, United Kingdom*
[c]*Institute of Physics, Khawaja Fareed University of Engineering and Information Technology, Rahim Yar Khan, Pakistan*
[d]*Department of Physics and Astronomy, College of Science, P.O. BOX 2455, King Saud University, Riyadh 11451, Saudi Arabia*
[e]*Department of Chemistry, College of Science, King Saud University, Riyadh 11451, Saudi Arabia*

The Y_2O_3 doped polypyrrole composites has been synthesized (PPy-Y_2O_3) through an in-situ polymerization route, to get dielectric properties for potential applications. XRD confirmed the formation of the composites. SEM confirms the flakier structure in the PPy-Y_2O_3. The impedance of pure Y_2O_3 ~ 14 Ω, PPy ~12 Ω to PPy-10%Y_2O_3 ~10 Ω compositesdecreased, signify the increase in AC conductivity of PPy-Y_2O_3. The temperature-dependent dielectric properties follow the Maxwell-Wagner model. AC conductivity of the PPy/Y_2O_3, increased with an increase in temperature depending on Jonscher's power law. Therefore, the present study suggested that PPy-Y_2O_3 composites can be considered useful for device applications.

(Received October 22, 2023; Accepted January 3, 2024)

Keywords: Dielectric spectroscopy, XRD, SEM, EIS

1. Introduction

In recent years, Yttrium oxide (Y_2O_3) rare earth metal oxide was extensively focused by researchers due to its wide applications in the field of device fabrication [1–3]. The Y_2O_3 is an outstanding ceramic material of excessive technological importance because of good corrosion resistivity, high melting point (2683 K), chemical stability as well and low instability in vacuum. Translucent yttria ceramics are valuable for optical applications, including waveguides for high-intensity discharge lamps, IR windows, and in laser as a host materials [4-6]. The crystal structure of yttria can be cubic (C-bixbyite type) but also exhibits hexagonal and monoclinic phases [7-8]. The cubic phase, stable at an ambient temperatures, melts at approximately 2400°C. This phase is chemically stable, possessing wide band gap of 5.5 eV and an extensive transparency range from 0.29 to 8 μm [9], and also displays rich oxygen vacancies on its surface. The Y_2O_3 has potential applications in both piezoelectric as well as semiconductor devices for example photodiodes, transparent electrodes, solar cells, and catalysts in addition to gas sensors [10-14]. Conversely, the conducting polymers have an extensive series of applications for instance sensors by sensing the vapor of different gases [15], Schottky diodes [16], field-effect transistors [17], and light-emitting diodes [18]. Among the family of many conducting polymers, PPy is known as positive conducting polymers widely used to synthesize composites owing to its simple synthesis, good compatibility, high electrical conductivity, and excellent ecological stability [19-20]. Its chemical formula is C_4H_4NH and the chemical structure of polypyrrole is exhibited in Figure 1. The electrical conductivity of polypyrrole can be improved by combining inorganic fillers [21], furthermore, the conductivity of polypyrrole depends on the dopant ions [22–24]. Several investigators have more

* Corresponding author: symali@ksu.edu.sa
https://doi.org/10.15251/JOR.2024.201.13

devotion to exploring the conducting polymer/inorganic-particle composites might show outstanding physical and mechanical characteristics [25].

Newly, PPy/inorganic-filler composites were synthesized utilizing metal oxides like, Fe_3O_4 [26], TiO_2 [27] MnO_2 [28], and Y_2O_3 [29] have been reported. The composites of polyaniline-yttrium oxide (PANI-Y_2O_3) were synthesized using chemical polymerization technique. Extensive research on these composites (PANI-Y_2O_3) has revealed a significantly high dielectric constant, suggesting potential applications in the fabrication of micro-electromechanical systems and charge-storage devices. This enhancement in the dielectric constant, facilitates an efficient charge transport mechanism as compared to pristine polyaniline. Such materials(PANI-Y_2O_3) have been pivotal in the development of next-generation dynamic RAM devices and actuators [30]. The polypyrrole-yttrium oxide (PPy-Y_2O_3) composites were prepared by chemical polymerization method using $FeCl_3$ as an oxidant agent. The resulting polypyrrole-yttrium composites are studied and can be suitable for the fabrication of sensors, actuators, and rechargeable batteries and also for many potential applications. The synthesized composite material performs good semiconductors as well as is very supportive to fabricate the electronic devices and their potential applications in technology [31]. In this work, low low-weight ratio of Y_2O_3 dopant was added to the polypyrrole to synthesize a PPy/Y_2O_3 composite through a chemical polymerization technique. The XRD, SEM, EIS, and dielectric spectroscopy techniques have been applied to examine the effect of Y_2O_3 on the Dielectric Characteristics of composite.

2. Experimental work

Pyrrole was bought from Riedel-de-Haen. Ammonium persulfate comes from Duksan chemicals. The Y_2O_3 was bought from UNI-CHcM chemicals and Hydrochloric acid was bought from Sacharlu. All material was employed conventionally excluding pyrrole. The chemical polymerization technique is utilized to synthesize polypyrrole in an open environment and APS is used as an oxidant.

The molar ratio of monomer to oxidant was kept 1:1. The required amount of APS was dispersed into 100 mL de-ionized water and strongly for 30 min at 25 ^{0}C. After that 3- mL of pyrrole was introduced into 100 mL de-ionized water and 5 mL HCl was presented dropwise to keep pH between 0–1. After 30 min, both solutions were mixed as well and stirred for 3 hours. the solution was left overnight in an open environment to achieve complete polymerization. Finally, got greenish-black solution was filtered with Wattman filter paper and then refined repeatedly with de-ionizing water to eliminate HCl from the solution. The suspension was located at 70°C in a vacuum oven to dehydrate and then ground to fine powder of polypyrrole was attained. The PPy/Y_2O_3 composite was synthesized in the same as the synthesis of polypyrrole has been discussed above.

X-ray powder diffraction (XRD) analysis was conducted on a Panalytical X-Pert PRO diffractometer utilizing CuKα source (λ = 1.54 Å, at 40 kV, and 2θ = 10 to 70°. Scanning electron microscopy (SEM) was performed using the EVO50 ZEISS instrument. Electrochemical impedance spectroscopy measurement was performed from 100 kHz to 0.1 Hz frequency range for an open circuit with AC perturbation of 5 mV. Temperature-dependent dielectric properties were evaluated on pellets formed by compressing the samples at 10-tons in a stainless steel die (4 mm in diameter and 1 mm thickness), by employed two-probe method across frequency range of 20 Hz to 1 MHz. The samples were interfaced with a Keithley 2400 electrometer and current source electrometer.

3. Results and discussion

3.1. Structural analysis

The XRD profile of PPy, PPy/Y_2O_3 composite, and pristine Y_2O_3-nanoparticles are represented in Fig. 1. The XRD spectra for PPy states the amorphous nature due to a broad peak was found from 17-22^0 in the 2θ range [32]. It is clear from the XRD profile, that the structure of Y_2O_3-particles is crystalline and all characteristic peaks define that Y_2O_3 is a cubic phase with JCPDS No.083-0927 [33]. Scherer's equation, employed to calculate the crystallite size of Y_2O_3

nanoparticles was found 95 nm [34]. The XRD spectra for the PPy/Y_2O_3 composite display the characteristic peaks not only for PPy but also for the pure Y_2O_3 as depicted in Figure 1. From this exploration, it was successfully confirmed that the synthesized composite is composed of Y_2O_3-particles and PPy in addition to an increase in crystallinity [35].

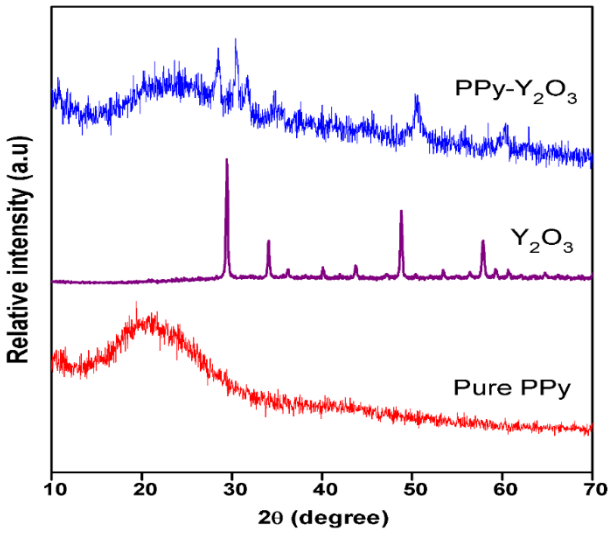

Fig. 1. XRD profiles for PPy, PPy/Y_2O_3 composite, and pure Y_2O_3.

3.2. Scanning electron microscopy (SEM) analysis

Fig. 2(a-b), exhibits SEM images of PPy-Y_2O_3 composite and pure Y_2O_3-nanoparticles. At high magnification, it was seen from SEM photo of PPy-Y_2O_3 composite is an expressive a hemi-spherical nature of polymer as clusters in composite which may be due to enhanced inter-chain interaction and results to increase the conductivity and flakier structure of pristine Y_2O_3. The Y_2O_3 particles are bound into the PPy chain because of the strong nanoparticle interaction. From this, it can be outcomes that the PPy-Y_2O_3 composite is seeing more improvement in particle dimensions as well as the flakier structure.

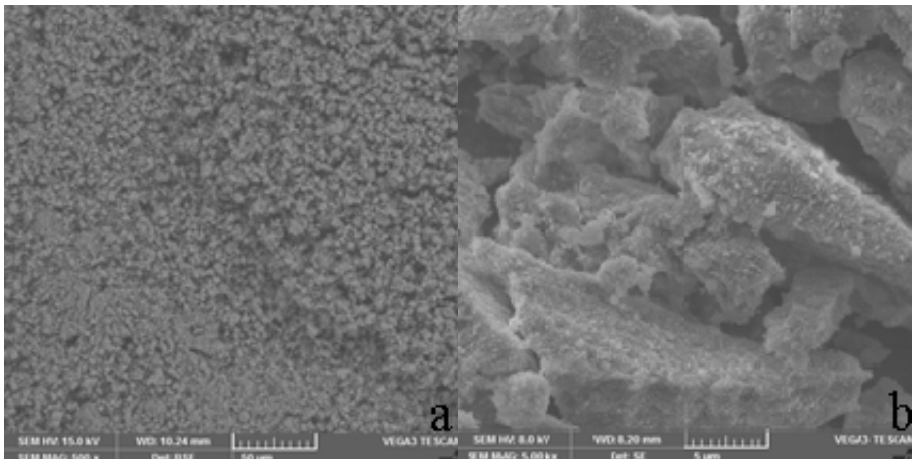

Fig. 2. SEM images of (a) PPy-Y_2O_3 composite (b) pure Y_2O_3.

3.3. Impedance analysis

The Nyquist plot for energy-packing devices contains vertical lines at high-frequency regions however, a semicircle made at a low-frequency region can display a decrease in electrical conductivity. A decrease in conductivity region recommends the interfacial charge transfer resistance [36]. The conductivity of an electrode material was determined by using an equivalent

series resistance (ESR) technique. The impedance of Y_2O_3 ~ 14Ω, PPy~12 Ω, and PPy/Y_2O_3 composite is found ~10 Ω. The impedance of composite is low as equated to Y_2O_3, in addition to pure PPy represents an increase in electrical conductivity owing to the accumulation of Y_2O_3 in the PPy matrix as depicted in Fig. 3. The PPy/Y_2O_3 composite is closely analogous to an ideal capacitor and has well-straight lines as compared to the others. The pure Y_2O_3, PPy, and PPy/ Y_2O_3 composite may have a semicircle at a high-frequency region which might expand the diffusion path length of ions and yield an obstacle to the motion of ions. The PPy/ Y_2O_3 composite may have a low impedance in its capacitance part which can exhibit better supercapacitor electrode material as compared to other electrode materials.

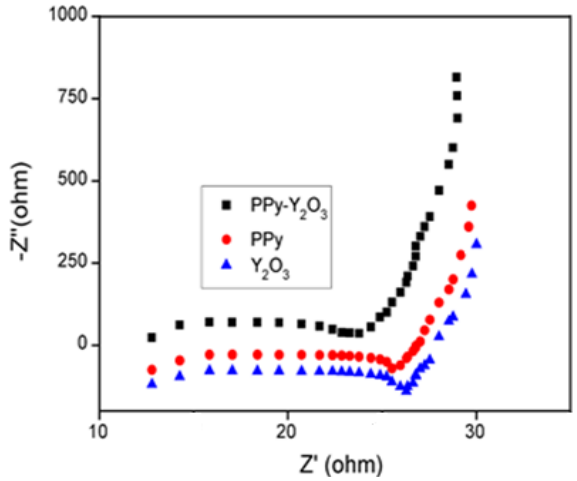

Fig. 3. Nyquist plot of PPy-Y_2O_3 composite, pure PPy and Y_2O_3 in 5 mV AC perturbations.

4. Temperature-dependent dielectric properties

4.1. Dielectric constant (ε′)

The dielectric constant was derived from the specified equation [37]. The variation of ε′ versus temperature at frequency 1MHz is depicted in Fig. 4. From the above figure, it appears that the growth in the temperature of the values of the dielectric constant enhances for all the measured samples. The various aspects are accountable for higher values of dielectric constant counting grain edge imperfections, oxygen voids, and interfacial dislocation pileup [38-39]. At high-temperature regions, an enhancement in the dielectric constant was seen at 1MHz frequencies. At high-frequency and temperature regions, the values of the dielectric constant are higher due to the polarization of arbitrarily oriented dipoles.

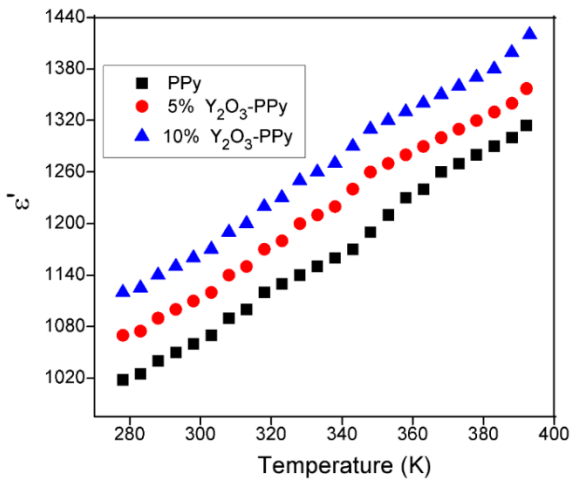

Fig. 4. Variation of ε′ versus temperature at frequency 1MHz for PPy, 5%Y_2O_3-PPy, 10%Y_2O_3-PPy composites.

4.2. Dielectric Loss (ε″)

Fig. 5, illustrates the variation of ε" with temperature at a frequency of 1MHz. As the temperature increases, ε" decreases, indicating the amount of energy dissipated within the dielectric under an applied AC field. In low-temperature regions, grain boundaries predominantly influence the behavior, leading to an observed increase in dielectric loss. However, at high-frequency and temperature regions, the electrons initially change their direction of motion at the grain boundaries owing to which the chance of arriving electrons towards the grain boundaries reduces consequently, the dielectric loss is decreased. So, it is clear that the abrupt increase in dielectric loss at low- low-temperature regions linked to interfacial polarization at the grain boundaries was distinguished. The large value of resistance was observed because of the insulating nature of the grain boundaries subsequently, much energy is needed for the exchange of electrons. Thus, a higher value of dielectric loss is recorded at low-temperature regions.

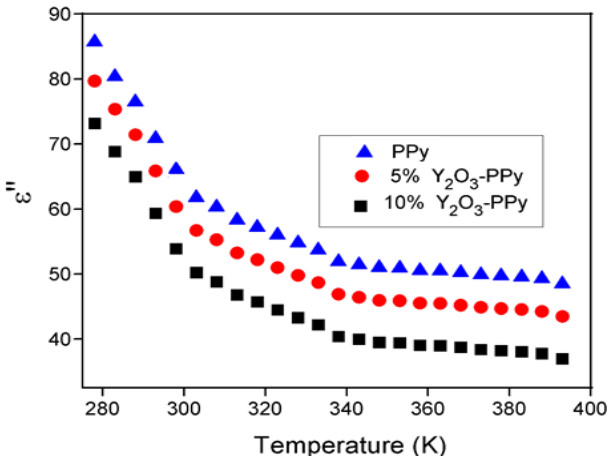

Fig. 5. Variation of ε" versus temperature at frequency 1MHz for PPy, 5%Y_2O_3-PPy, 10%Y_2O_3-PPy composites.

4.3. AC conductivity (σ_{AC})

The AC conductivity (σ_{AC}) for all samples was determined using the literature equation [40].

The variation in AC conductivity versus temperature at frequency 1MHz for all samples is depicted in Fig. 6(a-c). At high-frequency and temperature regions the hopping of polarons and bipolarons through the polymer chains was take place can be accountable for AC conductivity. Based on the Maxwell-Wagner model, the conducting grains in all samples are separated by notably resistive grain boundary layers [41]. The grain boundary effect diminishes the AC conductivity in regions of lower frequency and temperature. However, Jonscher's power law confirms the mutual connection between frequency and AC conductivity [42-43].

$$\sigma_{tot}(\omega) = \sigma_{DC} + A\omega^{n} \quad (1)$$

where, σ_{DC} represents the DC conductivity, n is a dimensionless fractional exponent, and A is the preexponential factor with units corresponding to electrical conductivity. As ‘n’ tends towards zero, the electrical conductivity converges to the DC conductivity and becomes independent of frequency. Therefore, the AC conductivity can be expressed as the sum of the DC conductivity and frequency-dependent AC conductivity. The results obtained from Fig. 6, it is confirmed that AC conductivity rises at a higher temperature and frequency region owing to the hoping of entombed charge carriers (polarons and bipolarons) through the conducting polymer chain [44]. Moreover, the values of dielectric constant (ε'), dielectric loss (ε"), and AC conductivity (σ_{AC}) are summarized in Table 1.

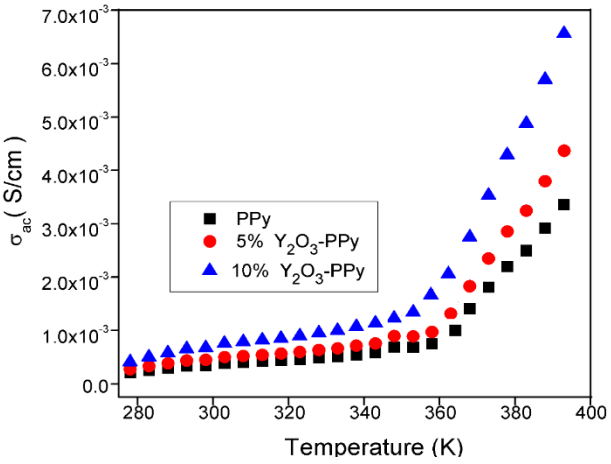

Fig. 6. Variation of AC conductivity versus temperature at frequency 1MHz for PPy, 5%Y_2O_3-PPy, 10%Y_2O_3-PPy composites.

Table 1. Temperature-dependent dielectric properties of PPy, 5%Y_2O_3-PPy, 10%Y_2O_3-PPy composites at 1-MHz frequency range.

Samples	**ε′ at 393K**	**ε″ at 393K**	**σ_{AC} (S/cm) at 393K**
PPy	1330	88	3.4×10^{-3}
PPy-5%Y_2O_3	1370	80	4.4×10^{-3}
PPy-10%Y_2O_3	1440	73	6.9×10^{-3}

5. Conclusions

Polypyrrole-doped Y_2O_3 was synthesized the PPy-Y_2O_3 composites by in-situ polymerization route. The structure of all the synthesized samples has been confirmed by X-ray diffraction analysis. The SEM also confirms the flakier structure in the PPy/Y_2O_3 composite. The impedance was calculated for pristine Y_2O_3 ~ 14 Ω, PPy ~12 Ω and PPy-10%Y_2O_3 composite are ~10 Ω. The temperature-dependent dielectric properties follow the Maxwell-Wagner model. The AC conductivity of all composites increases with an increase in temperature based on Jonscher's power law. Therefore, the synthesized composites can be considered useful for device applications and similarly for correlated fields.

Acknowledgements

The authors would like to acknowledge the Researcher's Supporting Project Number (RSP2023R113) King Saud University, Riyadh, Saudi Arabia, for their support in this work.

References

[1] Parker, I. D., Journal of Applied Physics, 75(3), 1656-1666 (1994); https://doi.org/10.1063/1.356350

[2] Jeon, H., Ding, J., Nurmikko, A. V., Xie, W., Grillo, D. C., Kobayashi, M., Otsuka, Applied physics letters, 60(17), 2045-2047 (1992); https://doi.org/10.1063/1.107109

[3] Rolo, A. G., Vieira, L. G., Gomes, M. J. M., Ribeiro, J. L., Belsley, M. S., Dos Santos, M. P., Thin solid films, 312(1-2), 348-353 (1998); https://doi.org/10.1016/S0040-6090(97)00233-2

[4] Johnson, R., Biswas, P., Ramavath, P., Kumar, R. S., Padmanabham, G., Transactions of the Indian Ceramic Society, 71(2),73-85(2012); https://doi.org/10.1080/0371750X.2012.716230

[5] Harris, DC, Infrared Phys Technol 39(4), 185-201(1998); https://doi.org/10.1016/S1350-4495(98)00006-1

[6] Ikesue, A., Aung, Y. L., Nature photonics, 2(12), 721-727(2008); https://doi.org/10.1038/nphoton.2008.243

[7] Skrikanth V, Sato A, Yoshimoto J, Kim J, Ikegami T, Crystal Res Technol 29(7), 981-984(1994); https://doi.org/10.1002/crat.2170290712

[8] Zhang P, Navrotsky A, Guo B, Kennedy I, Clark AN, Lesher C, Liu Q, J Phys Chem C 112(4), 932-938 (2008); https://doi.org/10.1021/jp7102337

[9] Hajizadeh-Oghaz, M., Razavi, R. S., Barekat, M., Naderi, M., Malekzadeh, Rezazadeh, Journal of Sol-Gel Science and Technology, 78, 682-691(2016); https://doi.org/10.1007/s10971-016-3986-3

[10] Heidari, Brown C, J Nanomed Res, 2(5), 20 (2015).

[11] Ferro, R., & Rodrıguez, J. A., Solar energy materials and solar cells, 64(4), 363-370 (2000); https://doi.org/10.1016/S0927-0248(00)00228-2

[12] Li, J., Ni, Y., Liu, J., Hong J., Journal of Physics and Chemistry of Solids, 70(9), 1285-1289 (2009); https://doi.org/10.1016/j.jpcs.2009.07.014

[13] Liu, Y., Zhang, Y. C., Xu, X. F., Journal of hazardous materials, 163(2-3), 1310-1314 (2009); https://doi.org/10.1016/j.jhazmat.2008.07.101

[14] Lu, H., Liao, L., Li, J., Wang, D., He, H., Fu, Q., Tian Y., The Journal of Physical Chemistry B, 110(46), 23211-23214 (2006); https://doi.org/10.1021/jp064079r

[15] Felix, J. F., da Cunha, D. L., Aziz, M., da Silva Jr, E. F., Taylor, D., Henini, M., de Azevedo, W. M., Radiation measurements, 71, 402-406(2014); https://doi.org/10.1016/j.radmeas.2014.05.014

[16] Koezuka, Tsumura A., Synthetic Metals, 28(1-2), 753-760 (1989); https://doi.org/10.1016/0379-6779(89)90600-0

[17] Gustafsson, G., Treacy, G. M., Cao, Y., Klavetter, F., Colaneri N., Heeger, A.J., Synthetic Metals, 57(1), 4123-4127 (1993); https://doi.org/10.1016/0379-6779(93)90568-H

[18] Chiang, J. C., MacDiarmid, A. G., Synthetic Metals, 13(1-3), 193-205 (1986); https://doi.org/10.1016/0379-6779(86)90070-6

[19] Jiang, G., Gilbert, M., Hitt, D. J., Wilcox, G.D., Balasubramanian, Appl. Sci and manufacturing, 33, 745 (2002); https://doi.org/10.1016/S1359-835X(01)00148-8

[20] Sailor, M. J., Ginsburg, E. J., Gorman, C. B., Kumar, A., Grubbs, R. H., Lewis, N. S., Science, 249 (4973), 1146-1149 (1990); https://doi.org/10.1126/science.249.4973.1146

[21] Li, L., Jiang, J., Xu. F., Materials Letters, 61(4-5), 1091-1096 (2007); https://doi.org/10.1016/j.matlet.2006.06.061

[22] Ayad, M. M., Zaki, E. A., European Polymer Journal, 44(11), 3741-3747 (2008); https://doi.org/10.1016/j.eurpolymj.2008.08.012

[23] Chung, S. F., Wen, T. C., Gopalan, Materials Science and Engineering: B, 116(2), 125-130 (2005); https://doi.org/10.1016/j.mseb.2004.09.023

[24] Long, Y., Chen, Z., Wang, N., Li, J., Wan, Physica B: Condensed Matter, 344(1-4), 82-87 (2004); https://doi.org/10.1016/j.physb.2003.09.245

[25] Roy, A. S., Anilkumar, K. R., Prasad, M. A., Journal of applied polymer science, 123(4), 1928-1934 (2012); https://doi.org/10.1002/app.34696

[26] Garcia, B., Lamzoudi, A., Pillier, F., Nguyen, H., Le, T., Deslouis, Journal of The Electrochemical Society, 149(12), B560 (2002); https://doi.org/10.1149/1.1517581

[27] Ferreira, C. A., Domenech, S. C., Lacaze, P. C., Journal of applied electrochemistry, 31, 49-56 (2001); https://doi.org/10.1023/A:1004149421649

[28] Yoneyama, H., Kishimoto, A., Kuwabata S., Journal of the Chemical Society, Chemical Communications, (15), 986-987 (1991); https://doi.org/10.1039/C39910000986

[29] Vishnuvardhan, T. K., Kulkarni, V. R., Basavaraja, C., Raghavendra, S. C., Bulletin of Materials Science, 29, 77-83 (2006); https://doi.org/10.1007/BF02709360

[30] Saeed, M., Shakoor, A., Ahmad, Journal of Materials Science: Materials in Electronics, 24 (9), 3536-3540(2013); https://doi.org/10.1007/s10854-013-1281-4

[31] Vishnuvardhan, T. K., Kulkarni, V. R., Basavaraja, C., Raghavendra, S. C., Bulletin of Materials Science, 29 (1), 77-83(2006); https://doi.org/10.1007/BF02709360

[32] Lian, M.; Wu, X.M.; Wang, Q.G.; Zhang, W.Z.; Wang, Ceram. Int. 43, 9877-9883(2017); https://doi.org/10.1016/j.ceramint.2017.04.171

[33] Gregory, N. W., Journal of the American Chemical Society, 79(7), 1773- 1774(1957); https://doi.org/10.1021/ja01564a077

[34]. A.L. Patterson, Phys. Rev. 56(10), 978 (1939); https://doi.org/10.1103/PhysRev.56.978

[35] Xia, H., Wang, Chemistry of Materials, 14(5), 2158-2165(2002); https://doi.org/10.1021/cm0109591

[36] Hu, L., Ren, Y., Yang, H., & Xu, Q., ACS applied materials & interfaces, 6(16), 14644-14652 (2014); https://doi.org/10.1021/am503995s

[37] Abbas, S.M., Dixit, A.K., Chatterjee, R., Goel, T.C., J. Magn. Magn. Mater. 309(1), 20-24 (2007); https://doi.org/10.1016/j.jmmm.2006.06.006

[38] Gandhi, N., Singh, K., Ohlan, A., Singh, D.P., Dhawan, S.K., Compos. Sci. Technol. 71(15), 1754-176 (2011); https://doi.org/10.1016/j.compscitech.2011.08.010

[39] Devi, D.S.P., Bipinbal, P.K., Jabin, T., Kutty, S.K.N., Mater. Des. 43, 337-347 (2013); https://doi.org/10.1016/j.matdes.2012.06.042

[40] Patil, R., Roy, A.S., Anilkumar, K.R., Jadhav, K.M., Ekhelikar, S., Compos. Part B 43, 3406-3411 (2012); https://doi.org/10.1016/j.compositesb.2012.01.090

[41] Gandhi, N., Singh, K., Ohlan, A., Singh, D.P., Dhawan, S.K., Sci.Technol. 71, 1754-1760 (2011); https://doi.org/10.1016/j.compscitech.2011.08.010

[42] Mangalaraja, R.V., Manohar, P., Gnanam, F.D., Awano, M., J. Mater. Sci. 39, 2037-2042 (2004); https://doi.org/10.1023/B:JMSC.0000017766.07079.80

[43] Aphesteguy, J.C., Jacobo, S.E., J. Mater. Sci. 42, 7062-7068 (2007); https://doi.org/10.1007/s10853-006-1423-7

[44] Ebrahim, S., Kashyout, A. H., & Soliman, M. Current Applied Physics, 9 (2), 448-454 (2009); https://doi.org/10.1016/j.cap.2008.04.007